THE DECAY OF HOMOGENEOUS TURBULENCE GENERATED BY MULTI-SCALE GRIDS

P. C. Valente*
Turbulence, Mixing and Flow Control Group, Department of Aeronautics
Imperial College London, London SW7 2AZ, United Kingdom
p.valente09@imperial.ac.uk

J. C. Vassilicos
Turbulence, Mixing and Flow Control Group, Department of Aeronautics
Imperial College London, London SW7 2AZ, United Kingdom
j.c.vassilicos@imperial.ac.uk

ABSTRACT

An experimental investigation of freely decaying homogeneous, quasi-isotropic turbulence generated by a low-blockage space-filling fractal square grid is presented. We find good agreement with previous work by Mazellier & Vassilicos ["Turbulence without the Richardson-Kolmogorov cascade", *Phys. Fluids* **22**, 075101 (2010)] but also extend the length of the assessed decay region and consolidate the results by repeating the experiments with a second probe of increased spatial resolution. It is confirmed that this moderately high Reynolds number turbulence ($150 < Re_\lambda < 400$) does not follow the classical high Reynolds number scaling of the dissipation rate $\varepsilon \sim u'^3/L$ which is in fact equivalent to a proportionality between the Taylor-based Reynolds number Re_λ and the ratio of integral scale L to Taylor micro-scale λ. Instead we observe a constant ratio L/λ whilst Re_λ decays during free turbulence decay. Alternative reasons for this non-classical behaviour are discussed, including various ways in which the turbulence may fall into a self-preserving, single-length-scale state. It is also shown that the measured 3D energy spectra can be reasonably collapsed using a single length-scale over the entire decay region even though the Reynolds number is high enough for conventional decaying turbulence to display spectra with two-scale (inner and outer) Kolmogorov scaling.

Introduction

The energy dissipation rate can be scaled with the large scale variables u' & L (the r.m.s. velocity fluctuation and the integral scale respectively) to give the dimensionless dissipation rate (Taylor, 1935):

$$C_\varepsilon(Re_\lambda, Re_0, *) \equiv \frac{\varepsilon L}{u'^3} \tag{1}$$

where C_ε is in general dependent on the local Reynolds number Re_λ (local as in particular to given stream-wise position aft of the grid in a wind-tunnel experiment) and on the initial conditions via their characteristic Reynolds number Re_0 and other topological details (represented by the asterisk). Nonetheless C_ε is expected to loose its Reynolds number dependence (Re_λ & Re_0) for sufficiently high Reynolds numbers, possibly retaining only information about the large scale flow topology (Mazellier & Vassilicos, 2008). Here we have chosen the Taylor micro-scale based Reynolds number $Re_\lambda = u'\lambda/\nu$ as the local Reynolds number (but the integral-scale based Reynolds number would be equally appropriate) and a grid Reynolds number $Re_0 = U_\infty t_0/\nu$ to be the initial conditions Reynolds number (t_0 was arbitrarily chosen to be the thickness of the largest bar of the grid).

The functional form of C_ε plays a fundamental role in determining the energy decay rate of the turbulent flow since it relates the energy dissipation ε with the kinetic energy ($u'^2/2$) and the 'eddy turn-over time' (L/u'). Together with an estimate of the growth of the integral scale (or the 'eddy turn-over time'), obtained for example from the conservation of invariants, the energy decay rate is completely determined, usually as a power law:

$$u'^2 = A(x - x_0)^{-n} \tag{2}$$

For example, assuming C_ε is constant and that either Loitsyanky or the Saffman invariants are finite and conserved during decay it follows that the power law decay exponents must be $n = 10/7$ and $n = 6/5$ respectively. Assuming, on the other hand, that $C_\varepsilon \sim Re_\lambda^{-1}$ during decay (as in self-preserving decaying turbulence where L/λ remains constant whilst Re_λ decays thus yielding $C_\varepsilon \sim Re_\lambda^{-1}$) the conservation of the same invariants yields $n = 5/2$ & $n = 3/2$ respectively. It is therefore clear that it's not possible to study the problem of the energy decay rate of freely decaying turbulence and its dependence on initial conditions without understanding the behaviour of C_ε during decay and its dependence on initial conditions.

*Acknowledges the support of the Portuguese Foundation for Science and Technology (grant SFRH/BD/1223/2009)

Note that, although $C_\varepsilon \sim Re_\lambda^{-1}$ is the functional form found in the 'final period of decay' where the non-linear energy transfer is negligible and consequently only direct dissipation via viscous diffusion at all scales is possible ($\varepsilon \sim \nu u'^2/L^2$ (Tennekes & Lumley, 1972)), this should not be confounded with, for example, self-preserving solutions of the Kàrmàn-Howarth equation (Kármán & Howarth, 1938) valid for high Reynolds number turbulence with non-negligible non-linear energy transfer (see e.g. Sedov, 1959; George, 1992; Mazellier & Vassilicos, 2010). The present experiments are just such an example of moderate to high Reynolds number turbulence (up to $Re_\lambda \approx 400$) with $C_\varepsilon \sim Re_\lambda^{-1}$.

Self-similar decay of homogeneous turbulence

Self-similar solutions of the spectral transfer equation (Lin, 1947):

$$\frac{\partial E(k,t)}{\partial t} = T(k,t) - 2\nu k^2 E(k,t) \tag{3}$$

can be sought in terms of a single determining length-scale $\ell(t)$ which is dynamically relevant at all scales of the flow (as opposed to two length-scales dynamically relevant for large and small scales separately). This can be expressed by the ansatz:

$$\begin{cases} E(k,t) = F(t, Re_0, \star) f(k\ell(t), Re_0, \star) \\ T(k,t) = G(t, Re_0, \star) g(k\ell(t), Re_0, \star) \end{cases} \tag{4}$$

which implies that the shapes of the dimensionless functions f & g remain unchanged while the turbulence decays, but nonetheless the shape of the spectra depend in principle on the initial conditions, denoted by '$\star$', and the initial conditions Reynolds number Re_0.

There are two main routes to obtain self-similar solutions depending on the choice of the scaling function G (George, 1992; Speziale & Bernard, 1992): either determine F and G directly from dimensional analysis and the assumption that they depend only on $u'(t)$ & $\ell(t)$, leading to $F = u'^2\ell$ and $G = u'^3$, which is the classical similarity constraint used e.g. by Kármán & Howarth (1938) and Sedov (1944, 1959); or relax this constraint and let the equation itself dictate the functional forms of G and F which turn out to be $G = \nu u'^2/\ell$ and $F = u'^2\ell$. The two routes lead to the same answer only if the Reynolds number $u'\ell/\nu$ remains constant during decay.

We follow Mazellier & Vassilicos (2010) and consider self-similar solutions of the type proposed by George (1992); George & Wang (2009), but we cannot preclude the possibility of the fractal generated flow achieving a self-similar state where the classical similarity constraint is satisfied as in Sedov (1944). This influences little the following discussions since we focus on consequences of self-similarity which are common to both similarity constraints, such as the proportionality between L and λ (and thus ℓ can be taken to be either L or λ) and the preservation of the shape of f normalised by u' & ℓ.

Mazellier & Vassilicos (2010) proposed a convenient functional form for the kinetic energy decay and the evolution of L & λ that is both consistent with the power-law decay

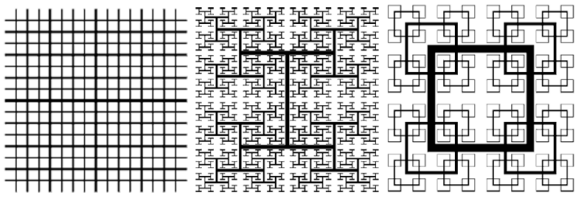

Figure 1. Three different fractal grids studied by Hurst & Vassilicos (2007). From left to right, a fractal cross grid, a fractal 'I' grid and a fractal square grid

and the exponential decay law proposed by George & Wang (2009):

$$\begin{cases} L^2 \propto \lambda^2 \propto \ell^2 = \ell(x_0)^2 \left[1 + \dfrac{4\nu ac}{\ell^2(x_0)U_\infty}(x - x_0)\right] \\ u'^2 = \dfrac{2u'^2(x_0)}{3}\left[1 + \dfrac{4\nu ac}{\ell^2(x_0)U_\infty}(x - x_0)\right]^{-(1+c)/2c} \end{cases} \tag{5}$$

where a and c are dimensionless positive real numbers ($a, c > 0$). In the limit of $c \to 0$ (5) asymptotes to an exponential decay with constant length-scales throughout the decay, but otherwise it is a power-law decay with an exponent $n = (1 + c)/2c$. This power law decay can also be written and fitted as

$$u'^2 \sim (x - \xi_0)^{-n} \tag{6}$$

where $\xi_0 = x_0 - \frac{\ell^2(x_0)U_\infty}{4\nu ac}$. Note that ξ_0 is not the conventional virtual origin where the kinetic energy is singular and that it does not have to be positive.

Multi-scale-grid generated turbulence

One of the motivations behind studying turbulence-generating grids with a fractal arrangement, such as the ones proposed by Hurst & Vassilicos (2007) (see Figure 1), is the expectation that these multi-scale turbulence generators will create a turbulent field with sufficiently different initial conditions to be noticeable, beyond experimental error, on turbulence properties such as the energy decay rate and dissipation scaling. Indeed their experimental results seem to confirm these expectations most dramatically for some of the grids, namely some of the fractal square grids, but not so significantly for other grid geometries like the fractal cross and 'I' grids (even though turbulence data generated with fractal cross and 'I' grids were use by Mazellier & Vassilicos (2008) to demonstrate and quantify the dependence of C_ε on large-scale flow topology).

To gain understanding of the differences between fractal and regular grid-generated turbulence as well as the differences between the three types of fractal grid turbulence generators proposed by Hurst & Vassilicos (2007) one needs to consider the turbulence generation mechanisms and how they may be affected by the fractal design. It is important to recognise two essential processes of homogeneous turbulence generation triggered by the upstream grid: i) the formation of shear layers on the solid boundaries leading to turbulent wakes

and ii) the interaction between adjacent turbulent wakes leading to the diffusion of inhomogeneities and the breakdown of these individual wakes. This latter mechanism is essential for the generation of a freely decaying homogeneous field instead of individual turbulent wakes developing downstream.

The turbulence generation mechanism of grids with a fractal design differ from non-fractal design not only by inducing wakes of different sizes behind each individual bar, but also for controlling the interaction between the similar size wakes and wakes of different sizes. For the turbulence downstream to become homogeneous with a high turbulence intensity it is important that: i) the fractal dimension of the grid takes the maximum possible value 2, ii) there are sufficient fractal iterations N (number of repetitions of the base geometry on different sizes) and iii) there is, in the case of fractal 'I' and square grids, a sufficiently large ratio between the thickness of the largest and smallest bars, $t_r = t_0/t_{N-1}$. From the accumulated experience from laboratory and numerical experiments since Hurst & Vassilicos (2007), namely Mazellier & Vassilicos (2010); Nagata *et al.* (2008); Laizet & Vassilicos (2011) it can be inferred that design parameters of the fractal grids must be carefully chosen if we are to expect a significant region of high Reynolds number homogeneous quasi-isotropic turbulence downstream from the grid. As a rule of thumb one needs at least $N = 4$ fractal iterations and a thickness ratio higher than $t_r = 10$.

Experimental data

A short outline of the experimental setup is given here, but the reader is referred to Valente & Vassilicos (2010) for a more complete account. These experiments were performed in an open circuit wind-tunnel with a square test section of side $T = 0.46m$ and $5m$ in length, where measurements were taken at the centreline from $x \approx 1.8m$ up to $x \approx 4.5m$. The data were taken with one- and two-component hot-wire anemometers operating in constant-temperature mode (CTA) using a DANTEC StreamLine CTA system. For the single component measurements two different single-wires (SW) were used with a sensing length (l_w) of $1mm$ & $0.45mm$ respectively. For the two component measurements a cross-wire (XW) with $l_w = 0.5mm$ was used. The tested fractal square grid, sketched on the right hand side of Figure 1, has $N = 4$ fractal iterations, a thickness ratio of $t_r = 17$ and a blockage ratio of $\sigma = 25\%$.

The present results are compared with the experimental investigation of Mazellier & Vassilicos (2010), which includes measurements in the same wind-tunnel using the same fractal square grid, but the length of the assessed decay region was limited to $x < 3.5m$. Their data were taken with SW sensors of $l_w = 1mm$ driven by the DISA 55M10 CTA bridge.

Energy decay One of the central properties of turbulence generated by the fractal square grids is the accelerated rate of decay. Previous studies suggested that the decay law might be exponential or as in (5) with a low value of c (and therefore a high value of n) (Hurst & Vassilicos, 2007; Mazellier & Vassilicos, 2010). In the present work we show that by increasing the length of the assessed decay region and by applying a wide range of fitting methods (see Valente & Vassilicos (2010) for details) we can distinguish between an

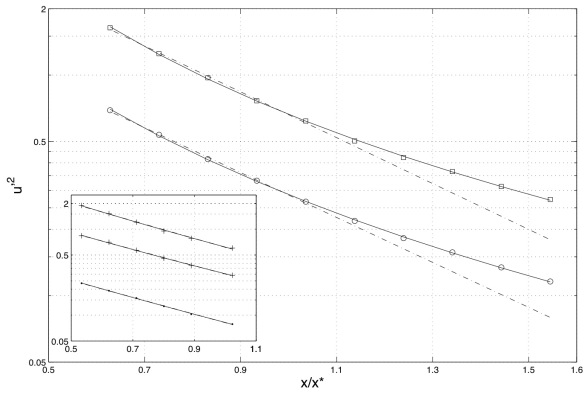

Figure 2. Turbulence decay for: $U_\infty = 10m/s$ (○); $U_\infty = 15m/s$ (□), fitted by the non-linear least squares fitting method used in Valente & Vassilicos (2010) (solid line) and by using (5) with a very low value of c as in Mazellier & Vassilicos (2010) dashed line. Insert shows the Mazellier & Vassilicos (2010) data for $U_\infty = 5, 10, 15m/s$ fitted with the same algorithms.

exponential and a power law decay and suggest that the turbulent kinetic energy decays as in (5) or equivalently (6) with an exponent n close to $n \approx 2.5$ (see Table 1). This is much less than the values of n reported by Mazellier & Vassilicos (2010) but nonetheless much larger than the exponents found for decaying turbulence generated by regular and active grids, typically $1.0 < n < 1.5$. In Figure 2 the decay of the longitudinal component of the turbulent kinetic energy is plotted against the streamwise position x normalised by the wake interaction length-scale $x_* \equiv L_0^2/t_0$ (L_0 is the side of the largest square of the fractal grid and t_0 is it's thickness). Linear abscissae vs. logarithmic ordinates are chosen so that an exponential decay yields a straight line. The data are fitted using (5) and a very low value of c (i.e. very high value of n) as in Mazellier & Vassilicos (2010) (dashed line) and also using a non-linear least-squares regression algorithm used in Valente & Vassilicos (2010) (solid line) which yields (5) or (6) with n close to 2.5. It can be appreciated that considering only the region $0.5 < x/x_* < 1$ the two fits appear equally valid, but by increasing the range to $x/x_* \approx 1.5$ the distinction between the two decay laws is clear (refer to Valente & Vassilicos (2010) for further discussions and details).

It is interesting to notice that the power law exponents obtained are close to 2.5 which is the value of n expected for decaying turbulence with conserved Loitsyansky invariant and $C_\varepsilon \sim Re_\lambda^{-1}$. For decaying turbulence with conserved Loitsyansky invariant and the assumption of self-similarity of large-scale motions we should have $u'^2 L^{M+1} = Const$ for $M = 4$. In Figure 3 this quantity is plotted and it can be seen that $u'^2 L^5$ is indeed approximately constant for much of the decay region when $U_\infty = 10m/s$, but much less so when $U_\infty = 15m/s$. However, n is not quite 2.5 either when $U_\infty = 15m/s$.

Dissipation scaling Another central property of turbulence generated by this fractal square grid is the fact

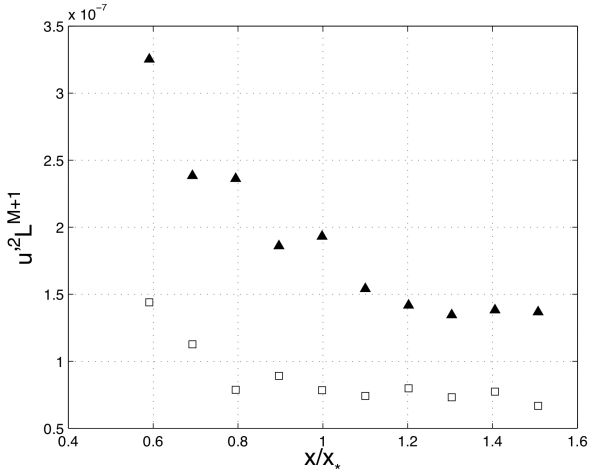

Figure 3. Development of $u'^2 L^{M+1}$ for $M = 4$ during decay for $U_\infty = 10m/s$ ($\square$); $U_\infty = 15m/s$ ($\blacktriangle$).

Table 1. Decay exponents and virtual origin estimation from the non-linear least-squares fitting method.

Grid	U	Power law	
	(ms^{-1})	n	$\xi_0(m)$
SFG	10	2.52	-0.89
SFG	15	2.36	-0.65

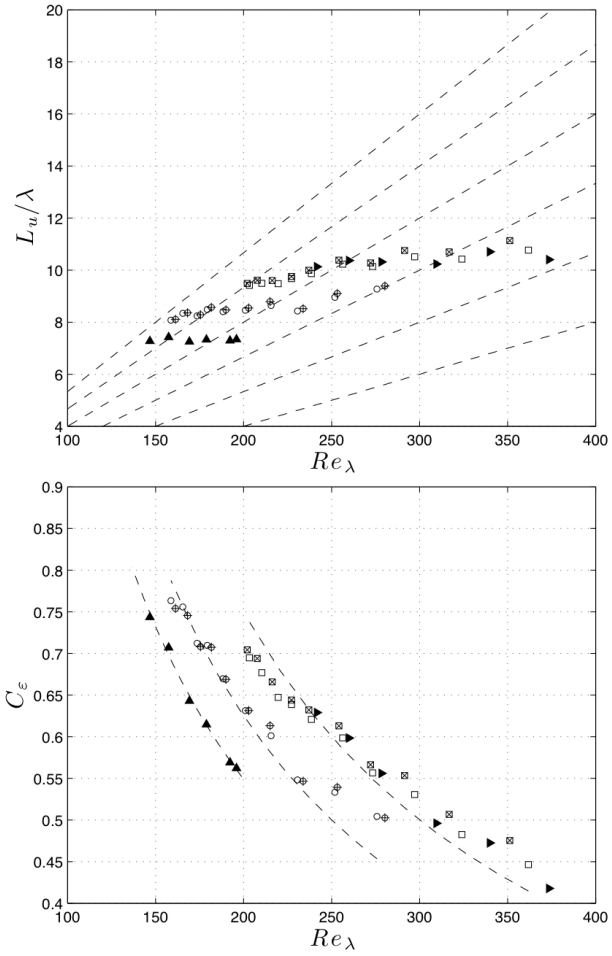

Figure 4. Behaviour of turbulence generated the multi-scale grid (SFG). Present data for two speeds and for two sensor lengths: $U_\infty = 10m/s$, $l_w = 1mm$ sensor $\bigcirc$; $U_\infty = 10m/s$, $l_w = 0.45mm$ $\otimes$; $U_\infty = 15m/s$, $l_w = 1mm$ $\square$; $U_\infty = 15m/s$, $l_w = 0.45mm$ $\boxtimes$. Data from Mazellier & Vassilicos (2010): $U_\infty = 5m/s$, $l_w = 1mm$ $\blacktriangle$, $U_\infty = 15m/s$, $l_w = 1mm$ $\blacktriangleright$. (a) Ratio between the integral scale L_u and the Taylor micro-scale λ contrasting with the expected classical high Reynolds behaviour $L_u/\lambda = \frac{C_\varepsilon}{15} Re_\lambda$ (dashed lines) for $0.3 < C_\varepsilon < 0.8$; (b) Normalised energy dissipation rate $C_\varepsilon = \varepsilon L_u / u'^3$.

that L_u/λ is (approximately) constant during decay and not proportional to Re_λ as in the Richardson-Kolmogorov phenomenology. It follows that the normalised energy dissipation for this flow takes the functional form $C_\varepsilon \sim Re_\lambda^{-1}$.

The experimental results are plotted in Figures 4a and 4b where it can be confirmed that in fact $L_u/\lambda \approx Const$ and $C_\varepsilon \sim Re_\lambda^{-1}$ for the entire decay region assessed in these measurements. These result are in quantitative agreement with previous experiments by Mazellier & Vassilicos (2010) although the larger length of the present wind-tunnel brings to evidence that L_u/λ is not exactly constant, but is roughly so for all the assessed decay region. This might be due to the wind-tunnel confinement affecting the growth of the integral scale L_u, since the ratio between the tunnel width T and L_u is decreasing both due to the growth in L_u and the growth of the side wall boundary layers which decrease the effective width of the tunnel. As this confinement effect might not affect the growth of λ as much as that of L_u, the ratio L_u/λ would decrease progressively downstream instead of being exactly constant, which is consistent with the experimental results. However, it may also be the case that a single-scale self-preserving turbulence obeying (4) and generated at sufficiently high Reynolds number may eventually collapse when a low values of Re_λ is reached which is nevertheless not low enough for the final period of decay to have set in.

The present results also confirm that the ratio L_u/λ is set by the grid Reynolds number (e.g. $Re_0 \equiv U_\infty t_0/\nu$ where U_∞ is the inflow velocity and t_0 is a characteristic length of the grid, here taken to be the thickness of the largest bars) as previously observed by Mazellier & Vassilicos (2010). Consequently, as the turbulence kinetic energy decays and Re_λ decreases, C_ε grows as Re_λ^{-1} but the proportionality factor in $C_\varepsilon \sim Re_\lambda^{-1}$ is pre-determined by the grid Reynolds number $Re_0 \equiv U_\infty t_0/\nu$. To illustrate that these results are not meaningfully influenced by the resolution of the probes, the measurements were repeated with a probe with twice the spatial resolution. It can be seen that the increased resolution probe ($d_w \approx 2.5\mu m$, $l_w \approx 0.45mm$) has a slightly higher L_u/λ ratio due to the better estimation of $\overline{(\partial u/\partial x)^2}$, but it does not change the main observation that L_u and λ are roughly constant during decay.

Collapse of 3D energy spectra The single-length-scale assumption which is in-built in the theory of self-similar decay of Sedov (1944, 1959) and George (1992); George & Wang (2009) can be assessed by plotting the normalised energy spectra for different positions along the mean flow direction and evaluating the collapse of the data or the lack thereof.

Here we present the 3D energy spectrum which is computed from two-component velocity signals. As it is argued in Valente & Vassilicos (2010) this provides a way to account for some of the anisotropy of the flow and thus obtain a more representative assessment of the spectral collapse. From the 3D energy spectrum we recovered the integral scale L (in an isotropic flow it is equivalent to the longitudinal integral scale L_u), the turbulent kinetic energy and the Taylor microscale. In Figures 5a & 5b we present the normalised energy spectra using large-scale variables u^2, L (Fig. 5a) and Kolmogorov inner variables ε, η (Fig. 5b) respectively. It can be appreciated that large-scale variables reasonably collapse the whole spectra (for both low and high wavenumber) whereas the Kolmogorov inner variables appear to collapse only the high wavenumber part of the spectra. Note that the uncertainty in estimating L as well as the ratio L/λ not being exactly constant are factors which can deteriorate the collapse which nonetheless appears to be reasonably good.

Conclusions

The decay of a fractal square grid-generated turbulence has been experimentally investigated using constant temperature hot-wire anemometry. This work complements previous research on the decay of fractal grid-generated turbulence (e.g. Hurst & Vassilicos, 2007; Mazellier & Vassilicos, 2010) by doubling the extent of the assessed decay region and by studying the effect of the hot-wire spatial resolution.

We find that for streamwise downstream positions beyond $x/x_* \approx 0.6$ the turbulence decays freely such that $L/\lambda \approx Const$ whilst Re_λ sharply decreases, at least up to the furthermost downstream position investigated. Nonetheless L/λ increases with increasing grid Reynolds numbers Re_0. These observations are in direct conflict with the Richardson-Kolmogorov cascade (Mazellier & Vassilicos, 2010), usually dominant at this range of Taylor-based Reynolds numbers Re_λ in regular grid- and active grid-generated turbulence.

We observe that the energy spectra for the present fractal square grid-generated turbulence are better described by a single-scale self-preserving form than by Kolmogorov (1941) phenomenology. Note that by Kolmogorov (1941) phenomenology we mean, not only the necessity of two dynamically relevant sets of variables, outer and inner, that collapse the low- and the high-frequency part of the spectra separately, but also that $L/\lambda \propto Re_\lambda$ and $C_\varepsilon = Const$, which implicitly dictates the rate of spreading of the high-frequency part of the spectra normalised by outer variables and vice-versa.

We also confirm the observations of Hurst & Vassilicos (2007) and Mazellier & Vassilicos (2010) concerning the abnormally high decay rates obtained for the fractal-square grids, compared with regular and active grid-generated turbulence. By having significantly extended the streamwise fetch of anemometry measurements we have been able to improve on Hurst & Vassilicos (2007) who found exponential decay,

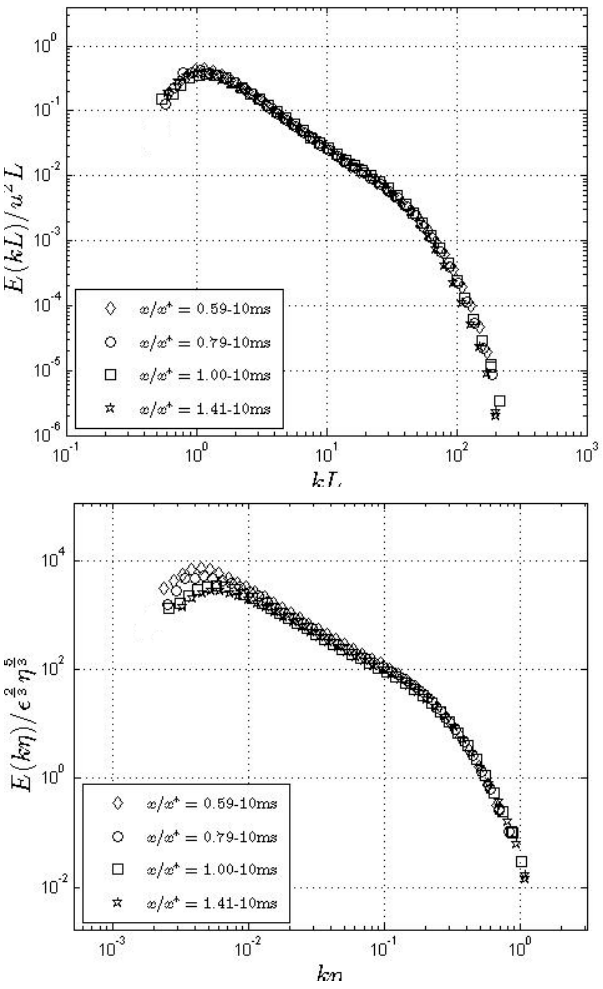

Figure 5. 3D energy spectra of turbulence generated by the fractal square grid at four streamwise downstream locations corresponding to $Re_\lambda = 275, 230, 200, 165$ at $U_\infty = 10ms^{-1}$ and normalized by (a) $\overline{u^2} = 2/3\overline{q^2}$ and L (b) η and ε.

i.e. (5) with $c = 0$, and on Mazellier & Vassilicos (2010) who found (5) with very small but non-zero values of c and therefore high values of n. Our data obtained over a much longer decay region support (5) and equivalently (6) with c such that n is close to 2.5 which is two to three times larger than the values found by Mazellier & Vassilicos (2010) but the n is nevertheless twice as large as the decay exponent of turbulence generated by regular and active grids.

REFERENCES

George, W. K. 1992 The decay of homogeneous isotropic turbulence. *Physics of Fluids A* **4** (7), 1492–1509.

George, W. K. & Wang, H. 2009 The exponential decay of homogeneous turbulence. *Physics of Fluids* **21**, 025108.

Hurst, D. J. & Vassilicos, J. C. 2007 Scalings and decay of fractal-generated turbulence. *Physics of Fluids* **19**, 035103.

Kármán, T. & Howarth, L. 1938 On the statistical theory of isotropic turbulence. *Proc. Roy. Soc. A* **164** (917), 192–215.

Kolmogorov, A. N. 1941 The local structure of turbulence in

incompressible viscous fluid for very large Reynolds. *CR Acad. Sci. URSS* **30**, 301.

Laizet, S & Vassilicos, J. C. 2011 Dns of fractal-generated turbulence. *Flow, Turbulence and Combustion* (In Revision).

Lin, CC 1947 Remarks on the spectrum of turbulence. In *First Symposium of Applied Mathematics, AMS*.

Mazellier, N. & Vassilicos, J. C. 2008 The turbulence dissipation constant is not universal because of its universal dependence on large-scale flow topology. *Physics of Fluids* **20**, 015101.

Mazellier, N. & Vassilicos, J. C. 2010 Turbulence without richardson-kolmogorov cascade. *Physics of Fluids* **22**, 075101.

Nagata, K., Suzuki, H., Sakai, Y., Hayase, T. & Kubo, T. 2008 DNS of passive scalar field with mean gradient in fractal-generated turbulence. *Int. Rev. Phys* **2**, 400.

Sedov, L. I. 1944 Decay of isotropic turbulent motions of an incompressible fluid. *Dokl. Akad. Nauk SSSR* **42** (3).

Sedov, L. I. 1959 *Similarity and Dimensional Methods in Mechanics, 2nd ed.*. Academic Press, New York.

Speziale, C. G. & Bernard, P. S. 1992 The energy decay in self-preserving isotropic turbulence revisited. *J. Fluid Mech.* **241**, 645–667.

Taylor, G. I. 1935 Statistical theory of turbulence. *Proc. R. Soc. London* **151** (873), 421–444.

Tennekes, H. & Lumley, J. L. 1972 *A First Course in Turbulence*. MIT Press, Cambridge, New York.

Valente, P. C. & Vassilicos, J. C. 2010 The decay of homogeneous turbulence generated by a class of multi-scale grids. HTTP://arxiv.org/abs/1101.0709.